Biosensors and Bioelectronics 42 (2013) 273–279

Contents lists available at SciVerse ScienceDirect

Biosensors and Bioelectronics

journal homepage: www.elsevier.com/locate/bios

Synthesis of a conductive network of crosslinked carbon nanotube/hemoglobin on a thiol-modified Au Surface and its application to biosensing

A.K.M. Kafi *, Maxwell J. Crossley

School of Chemistry, the University of Sydney, NSW 2006, Australia

ARTICLE INFO

Article history:
Received 26 July 2012
Received in revised form
25 September 2012
Accepted 10 October 2012
Available online 22 October 2012

Keywords:
Hemoglobin
Carbon nanotube
Three-dimensional networks
Electrical contact
H_2O_2 sensing

ABSTRACT

The synthesis of a network of crosslinked carbon nanotube/hemoglobin (CNT/Hb) on a thiol-modified Au surface and its use as sensor for H_2O_2 is reported. The constructed CNT/Hb 3-D network exhibits high conductivity by expediting the electrical transfer from Hb to the Au electrode and has a high electrocatalytic property for sensing hydrogen peroxide (H_2O_2). CNTs were first oxidized by treatment with concentrated nitric acid for 10 h and functionalized by reaction with the thiol group of 4-aminothiophenol and Hb was also reacted with 4-aminothiophenol. These modified CNTs and modified Hb were immobilized on a 4-aminothiophenol monolayer-modified Au electrode by co-electropolymerization by repetitive cyclic voltammetry scans ranging between −0.1 and +1.1 V (versus Ag/AgCl). Cyclic voltammogram (CV) and amperometry were employed to study electrochemical properties of the modified electrodes. Direct electrical communication between the redox center of Hb and an Au electrode was established through 3-D network of crosslinked CNT/Hb. The Hb present in the 3-D CNT/Hb network exhibited a pair of quasi-reversible redox peaks with a midpoint potential of −0.225 V and −0.075, cathodic and anodic respectively. The electron transfer rate constant, K_S and electron transfer co-efficient α were found to be 0.51 s^{-1} and 0.58, respectively. The modified electrode was used as a biosensor and exhibited a high sensitivity, long linear range and lower detection limit to H_2O_2, under optimal conditions. The apparent Michaelis–Menten constant (K_m) and Hb adsorption in the CNT/Hb network with average surface coverage of were found to be 0.19 mM and 4.8×10^{-10} mol cm^{-2}, respectively. This system should be very useful for other sensing applications.

1. Introduction

A fundamental requirement of any biosensor/bioelectronics system is to establish electronic coupling and good communication between the biomolecules (e.g., enzyme, protein) and the electronic supports (electrode). The sensing principle of such a bioelectronics device is based on the ability of the enzyme to catalyze a selective transformation of a specific substrate. The information then has to be conveyed to the read-out component of the system as an electrical signal. Electrical contact between biomolecules (e.g., redox enzyme) is the challenging task since the redox centers of the enzyme are located deep inside the insulated shells. The lack of good electrical communication between the biomaterial components and the electronic elements has been a major obstacle in a number of recent studies (Wang, 2008; Willner and Katz, 2005; Liu et al., 2007). Therefore, the main issue in bioelectronics is to ensure the electrical coupling of biomolecules with electrodes to facilitate direct electron exchange and that is the challenge addressed in the present work.

Direct electrical wiring between electron-relay modified enzymes and metal electrodes has opened a new route to biosensor and bioelectronics devices and to the direct electrochemical synthesis of biochemicals is the fundamental interest of many researchers (Wiilner et al., 1997). Since redox enzymes do not exchange electrons with simple metal electrodes in homogenous solution, a special fabrication is required to flow current through metal electrodes. Several techniques have been proposed to establish the electrical communication between the redox center of an enzyme and conventional metal electrodes (Raitman et al., 2002; Wang et al., 2006; Yan et al., 2008). In order to fabricate highly sensitive biosensor devices, the generation of high turnover rates between the redox enzyme and electrode surface is very important. Unfavorable orientation or direct adsorption of biomolecules onto a metal electrode surface may dramatically lower their catalytic activity, limitating the charge transport across matrices (Zhang and Li, 2004). In this context, controlled orientation of redox enzyme on an electrode surfaces and their effective electrical wiring have been demonstrated by the application of the reconstitution technique

* Corresponding author. Tel.: +61 2 9351 395151; fax: +61 2 9351 3329.
E-mail address: kafiakm@chem.usyd.edu.au (A.K.M. Kafi).

0956-5663/$ - see front matter © 2012 Elsevier B.V. All rights reserved.
http://dx.doi.org/10.1016/j.bios.2012.10.040

(Holland et al., 2011; Zayats et al., 2008; Willner et al., 2009; Fruk et al., 2009). Based on the reconstitution method, the electrical wiring of redox enzyme was accomplished with relay cofactor, metal nanotube/cofactor or nanoparticle/cofactor monolayer-functionalized electrode (Willner and Willner, 2001; Katz et al., 1997; Xiao et al., 2003; Patolsky et al., 2004; Holland et al., 2011). In spite of achieving high electron-transfer turnover rates in those systems, the forming of monolayer of enzyme on the surface of electrodes is a major disadvantage to the method, as a result of the low content of enzyme associated with the surface. All of these results come from the weak contact of the biomolecules to the electrode which causes the low electrical communication for biosensors.

One attractive solution to overcome all of those drawbacks is the use of nanomaterials to give 3D structure to biomolecules for electronic coupling and communication between the biomolecules and the electrode (Yehezkeli et al., 2009). For example, Willner et al. have demonstrated an excellent method to generate three-dimensional electrically wired Glucose Oxidase (GOD) electrodes that showed high electron-transfer turnover rates (Baravik et al., 2009). In this system, thioaniline-modified GOD in the presence of thioaniline-functionalized carbon nanotube (CNT) has created a three-dimensional bis-aniline-crosslinked CNT/GOD network. The resultant bis-aniline crosslinked network was redox active and able to medicate the electron from redox site of GOD to the base electrode. However, in spite of the successful demonstration of GOD wiring with electrode, there is no report on effective creation of a Hemoglobin (Hb)/CNT 3-D network. Nanoscale surfaces such as nanotubes or nanoparticles can overcome some limitations because they contain regions of high curvature that energetically limit biomolecules adsorption, and reduced steric hindrance of the substrate to binding site on the enzyme. The unique electrical properties, high chemical stability and high surface-to-volume ratio of carbon nanotubes have been intensively used for studying electron transfer of enzyme/protein for biosensor design and other purposes (Gooding et al., 2003; Yang et al., 2007; Sardesai et al., 2011). The ability of CNT to promote the electron-transfer reactions of enzyme such as Horseradish peroxidase (HRP) and hydrogen peroxide (H_2O_2) suggests great promise for enzyme-based amperometric biosensors (He and Dai, 2007). Redox enzymes can be immobilized on CNT with enhanced retention of their biocatalytic activity and used different biosensor devices by associating with transistors and electrode (Gooding et al., 2003). CNTs functionalized with redox enzyme associated with electrodes show high surface areas, effective charge transport and good electrical contact and led to use in biosensing and biofuel cell (Yehezkeli et al., 2009; Wang, 2005a,b). Biosensors have major advantages over traditional analytical methods, which has resulted in their more pronounced use in the biomedical and environmental fields (Wang et al., 2005). Significant progress has been made in the development of sensors, particularly in terms of sensitivity, selectivity, stability and simplicity (Dorst, et al., 2010; Kafi et al., 2008, 2010; Ligler, 2009; Kotani et al., 2011).

Herein, we have focused on a construction of three-dimensional (3-D) conductive Hemoglobin network with CNT onto the thiol-modified gold (Au) electrode. In order to obtain the 3-D network, CNTs modified with electropolymerizable aniline and 4-aminothiophenol-modified Hemoglobin were coelectroplolymerized on the thiol-modified Au electrode surface. Our results show that the created 3-D CNT/Hb composite effectively builds a good electrical communication between the redox centers of the Hb and an electrode. We have also evaluated the resultant 3-D CNT/Hb network in H_2O_2 biosensing as the sensitive and accurate H_2O_2 detection is of great interest to researchers because of its importance in the pharmaceutical, clinical and industrial settings (Wang and Wang, 2004).

2. Experimental

2.1. Reagents and materials

Hemoglobin was purchased from Sigma, used as received and stored at 4 °C. *N*-(ε-Maleimidocaproyloxy) sulfosuccinimide ester (sulfo-EMCS) was purchased from PIERCE (Through Thermofisher). Single-walled carbon nanotubes, 4-aminothiophenol, 1-(3-dimethylaminopropyl)-3-ethylcarbodiimide hydrochloride (EDC) were purchased from Aldrich. *N*-hydroxysulfosuccinimide sodium salt (NHS) was obtained from Sigma. 30% Hydrogen peroxide was bought from Fluka and the stock solution of H_2O_2 was diluted from this. All experimental solutions were prepared fresh by appropriate dilution of the stock solutions. All other reagents were of analytical grade and used as supplied. The pure water (18 MΩ cm) used to prepare all solutions in this study was purified with the Nanopure® water system. All experiments were performed in 0.1 mol l^{-1} phosphate buffer solutions (PBS) whose pH values were adjusted with K_2HPO_4 and KH_2PO_4.

2.2. Modification of Hb

Hemoglobin was functionalized based on the method described elsewhere (Baravik et al., 2009). Hb (50 mg) was dissolved in 0.1 M phosphate buffer (3 mL, pH 7.4). The solution was then be treated with *N*-(ε-Maleimidocaproyloxy) sulfosuccinimide ester (sulfo-EMCS) and stirred for 40 min. Then the solution was mixed with 4-aminothiophenol (thioaniline) and left for 2.5 h. Finally, the solution was eluted through a G-25 column (GE Healthcare) with 0.1 m phosphate buffer (pH 7.4) as the eluent. The resulting purified, functionalized Hb solution was lyophilized to yield a powder that was stored at −20 °C.

2.3. Modification of CNT

Prior to modification, CNTs were sonicated for 10 h in a mixture solution of concentrated sulfuric acid and nitric acids (3:1), resulting the oxidization of CNTs. The oxidized CNTs were washed with water and centrifuged several times to a final pH of 7.0. The CNTs were then reacted with a HEPES buffer, 0.01 M, pH=7.4, containing 2-(4 aminophenyl)-ethylamine and was stirred with 1-(3-dimethylaminopropyl)-3-ethylcarbodiimide hydrochloride (EDC) and *N*-hydroxysulfosuccinimide sodium salt (NHS) for 2 h at room temperature. Finally, the modified CNTs were thoroughly rinsed with water and centrifuged, at least four times, using a PBS solution.

2.4. Formation of 3-D CNT/Hb network on 4-aminothiophenol-modified Au

A gold (Au) electrode (2 mm diameter) was used in the formation of 3-D CNT/Hb network for this work. At first, the Au electrode was electrocycled ranging between −0.1 and +1.1 V (versus SCE) in solution containing H_2SO_4 to remove any contaminations and immersed in ethanol before monolayer assembly. The cleaned Au-electrode was modified by immersion in a solution of 50 mM thioaniline in ethanol. After 24 h to ensure a complete coverage, the Au electrode was thoroughly rinsed with ethanol and dried under a stream of nitrogen. This modified Au-electrode was then electropolymerized with modified CNTs and Hb in 0.1 M phosphate buffer (pH 7.4) by using a fixed number of repetitive cyclic voltammetry scans, ranging between −0.1 and +1.1 V (versus SCE), at a scan rate of 100 mV s^{-1}. The resulting modified Au electrode is denoted below as Au/SAM/CNT/Hb. For comparison, another electrode Au/SAM/Hb was also modified.

2.5. Instrumentations and measuring procedures

Electrochemical experiments were performed using a CHI (660B) workstation. Cyclic voltammetry and amperometric experiments were carried out in a conventional one-compartment cell with a three-electrode configuration holding 20 ml of supporting electrolyte (phosphate buffer). Three electrodes consist of the Au/SAM/CNT/Hb electrode or the Au/SAM/Hb electrode as the working, a platinum coil as a counter electrode, and a KCl saturated Ag/AgCl electrode as a reference electrode. Amperometric measurements were performed in a stirred cell by applying a potential of −0.4 V to the working electrode. A magnetic stirrer was used for this experiment. Prior to measurements, all electrolytes were deoxygenated by bubbling ultra-pure nitrogen for 30 min. All measurements were performed at room temperature.

3. Results and discussion

3.1. Schematic diagram of construction of the 3-D CNT/Hb network

Scheme 1 shows the schematic illustration of the procedures to assemble the CNT/Hb composite electrode. At first, 4-aminothiophenol was attached to Hb with the primary modification of the lysine residue of the Hb with the bifunctional *N*-(ε-Maleimidocaproyloxy) sulfosuccinimide ester (sulfo-EMCS), followed by the substitution of the maleimide residue with 4-aminothiophenol (a). Single-wall carbon nanotubes were carboxyl functionalized in a mixture of HNO_3 and H_2SO_4 for 10 h. This functionalized CNTs were then covalently coupled to 2-(4 aminophenyl)-ethylamine (b) using the water-soluble carbodiimide, (1-(3-(dimethylamino)propyl)-3-ethylcarbodiimide hydrochloride, EDC), to promote amide linkages between the carboxyl-terminated CNTs and the amine group of 2-(4 aminophenyl)-ethylamine. Proteins have many NH_2-containing groups in the side chains of their polypeptide backbones. Therefore, considering the strong amide-bonding interaction between carbonyl and NH_2 groups, functionalization of Hb was first done by the interaction between NH_2 group of Hb and COOH group of bifunctionalized *N*-(ε-Maleimidocaproyloxy)sulfosuccinimide ester (sulfo-EMCS). Finally, co-electropolymerization of aniline modified-CNTs and the 4-aminothiophenol modified-Hb onto the 4-aminothiophenol self assembled monolayer (SAM) on Au electrode was carried out in 0.1 M phosphate buffer (pH 7.4) by using a fixed number of repetitive cyclic voltammetry scans, ranging between −0.1 and +1.1 V (versus SCE), at a scan rate of 100 mV s^{-1} (Scheme 1B).

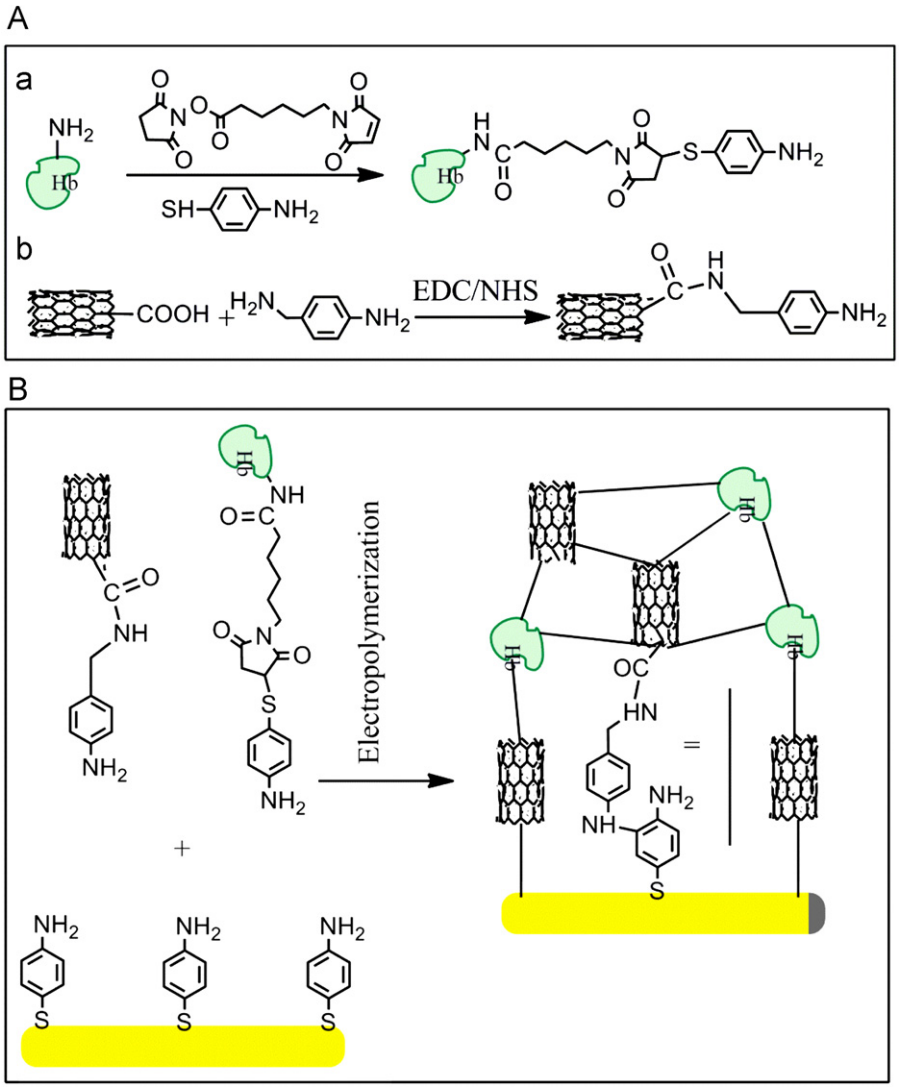

Scheme 1. A. (a) Modification of enzyme (Hb) with the polymerizable 4-aminothiophenol functionality. (b) Functionalization of the CNT with the electropolymerizable aniline functionality. B. Formation of the three-dimensional (3-D) oligoaniline-cross-linked CNTs/Hb composite by the co-electropolymerization of the thiol-modified Hb and thiol-modified CNT on the thiol-monolayer-functionalized Au electrode.

3.2. Direct electron transfer from Hb

To enable electron transfer from redox centers of enzymes to metal electrodes a monolayer of tightly bound proteins has been used (Willner and Katz, 2005). In this context, the covalent attachment of electron relays to layered enzyme electrodes provided a means to facilitate electrical communication between the enzyme layer(s) and the electrode, and to electrically activate the biocatalyst. However, most of those studies were based on the direct enzyme immobilization technique or termed as a two-dimensional (2-D) formation of enzyme. In the case of covalent attachment of enzyme, some electron relay units are close to redox active center of enzyme, which showed high effective electrical contact, while some electron relay units are in a remote position with respect to redox active center, resulting inefficient connecting to the electrode (Yan et al., 2008). Therefore, as a result, the observed net catalytic currents are lower due to different electrical wiring efficiencies. Although high electron-transfer turnover rates were observed in those systems, the unfavorable orientation of enzyme showed caused only a small amount of enzyme to be associated with the surface, causing the low electrical communication for the resultant biosensors. In the present work, bis-aniline bridge units are highly redox active, and CNTs played an anchor role 3-D CNT/Hb networks, the electron transfer rate from Hb to base electrode will be higher, and thus more sensitive, than in systems previously studied (Yan et al., 2008).

In order to investigate the direct electrochemistry attributed to Hb in 3-D CNT/Hb networks, cyclic voltammograms (CV) of the different electrodes recorded in a potential range between −0.5 and 0.2 V with pH 7.0 PBS at scan rate of 0.05 V/s. The resulting CVs are shown in Fig. 1. As we can see, no voltammetric peak was observed at the bare Au and thiol-modified only Au electrodes in the selected potential range. A small nearly irreversible reduction peak of the Hb takes place at the Au/SAM/Hb electrode in the same potential range. Interestingly, a well defined reversible redox peak was observed at the Au/SAM/CNT/Hb electrode, located at about −0.225 and −0.075 V, cathodic and anodic respectively. Therefore, the redox peaks of the Au/SAM/CNT/Hb are attributable to the electrochemical reaction of hemoglobin. In addition, all electroactive heme proteins at CNT/Hb networks have been reduced on the forward cathodic scan, with full conversion of the reduced proteins back to their oxidized forms on the reversed anodic scan. The formal potential E_0 [$E_0=(E_{pa}+E_{pc})/2$]of Hb in CNT/Hb networks was calculated to be −0.15 V which is assigned to the heme Fe(III)/Fe(II) transition. The peak to peak potential separation (ΔE_p) and the ratio of redox peak current (I_{pa}/I_{pc}) were found to be 0.15 V and approximately 1, respectively. Therefore, all the results indicated that Hb creates a three-dimensional network with CNTs in order to make an electrical communication between the redox centers of this Hb and the electrodes, and direct electron transfer of Hb in the CNT/Hb networks was achieved.

To further investigate the Hb characteristics at the CNT/Hb networks, the effect of scan rates on the Hb voltammetric behavior was studied in detail. Fig. 2A shows the CVs of the Au/SAM/CNT/Hb electrode at different scan rates in pH 7.0 PBS. As we can see, with the increase of the scan rates anodic and cathodic peak current increase gradually. As shown in Fig.2B, the peak currents were found to increase linearly with scan rate in the range from 0.05 to 0.25 V/s. This phenomenon suggested that the redox process of Hb was a surface-controlled and the Hb in 3-D network was highly efficient. According to the following equation: $Q=nFA\Gamma$, the average surface concentration of electroactive species can be calculated, where Q is the charge passing through the electrode with full reduction of electroactive Hb in CNT/Hb s networks, n is the number of electron, F is Faraday's constants and A is the surface area of electrode (Bard and Faulkner, 1980). The average surface concentration of electroactive Hb calculated from our experimental results was approximately 4.8×10^{-10} mol cm^{-2}. This value was more than that of the theoretical monolayer coverage, suggesting that more than one layer

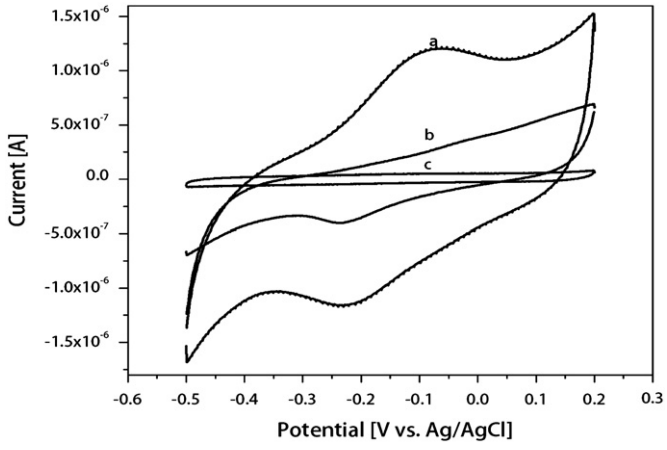

Fig. 1. Cyclic voltammetry of the different electrodes in 0.1 mol l^{-1} PBS with pH 7.0 at a scan rate of 0.1 V/s. (a), Au/SAM/CNT/Hb; (b), the Au/SAM/Hb and (c), bare Au electrode).

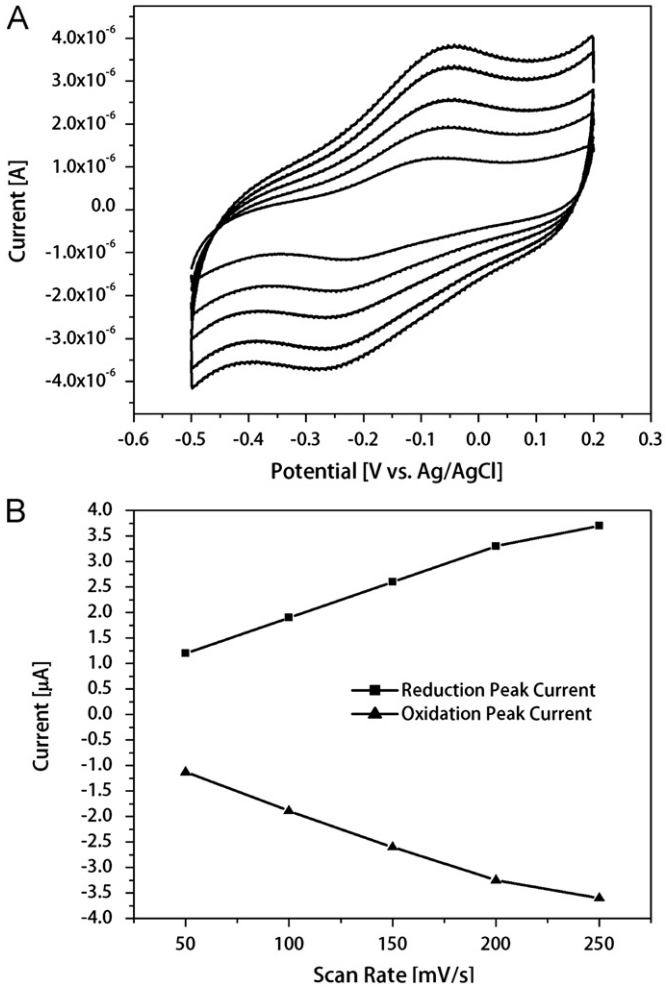

Fig. 2. (A) CVs of the Au/SAM/CNT/Hb electrode with different scan rates in 0.1 mol l^{-1} PBS with pH 7.0. The scan rates were from 0.05 to 0.25 V/s. (B) Reduction and oxidation peak current versus scan rates based on Fig. 2A.

of Hb was participating in the electron transfer process (Yang et al., 2011).

In order to calculate the electrochemical parameters, the relationship of the peak potential with scan rate was further constructed. Fig. S1 (in supplementary materials) shows the cathodic peak potentials versus natural logarithm of scan rate ($\ln v$). Since the peak potentials are shifted by changing the scan rate, this is a quasi-reversible electrode reaction driven by adsorption. According to following equations (Laviron, 1979)

$$E_p = E_0 + \frac{RT}{\alpha nF}\ln\frac{RTK_s}{\alpha nF} - \frac{RT}{\alpha nF}\ln\upsilon \quad (1)$$

Where α is the electron transfer coefficient, n is the electron transfer number, K_s is the standard electron transfer rate constant, υ is the scan rate, E_0 is the formal potential and R, T and F are gas, temperature and the Faraday's constant. As we can see the relationship between E_p versus $\ln\upsilon$ is linear as $E_p(V) = -0.32 - (-0.043)x$, the αn is calculated to be 0.58 from the slope. Therefore, given $0.3 < \alpha < 0.7$ in general it could be determined that $n=1$ and electron transfer co-efficient $\alpha = 0.58$ (Ma et al., 2000). Therefore, it can be concluded that the redox reaction between Hb and the Au electrode is a single electron process. Then, electron transfer rate constant, K_s value is calculated to be 0.51 s^{-1}, as the intercept of E_p and formal potential E_0 are known.

3.3. Electrocatalytic activity towards H_2O_2

In order to apply CNT/Hb network in biosensing, the electrocatalytic activity of the modified electrode was studied towards H_2O_2. The cyclic voltammograms of the Au/SAM/CNT/Hb electrode, in PBS at pH 7.0, in the presence and the absence of H_2O_2 are shown in Fig. 3. As we can see, as soon as H_2O_2 was added in electrolyte solution, compared with the system with no H_2O_2 present, an obvious increase in the reduction peak was observed with the disappearance of the oxidation peak. This result suggests that Hb in the CNT/Hb networks retains its bioactivity and catalyzes the reduction of H_2O_2 (Turner, 2007). The generic reaction of the immobilized Hb to H_2O_2 reduction can be explained by the following scheme (Kafi et al., 2008).

$$\mathrm{HbFe(III)} + \mathrm{H_2O_2} \rightarrow \mathrm{Compound\ I\ Fe\{(IV)=O\}} + \mathrm{H_2O} \quad (2)$$

$$\mathrm{Compound\ I\ Fe\{(IV)=O\}} + 2e + 2H^+ \rightarrow \mathrm{HbFe(III)} + \mathrm{H_2O} \quad (3)$$

According to the above reaction, the added H_2O_2 increases the oxidation form of the heme group of Hb in the proximity of the electrode, resulting in increased cathodic current and the disappearance of the anodic current.

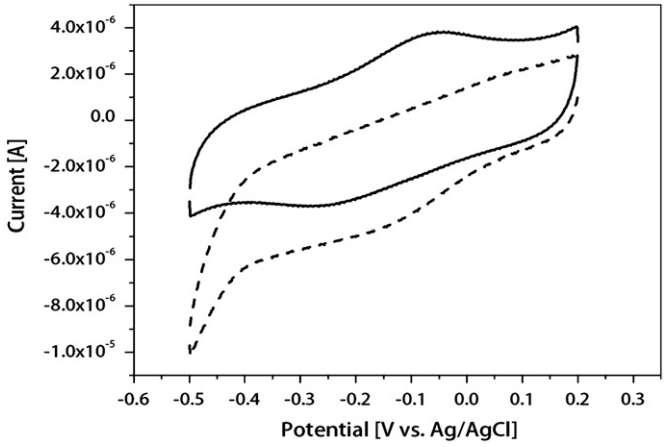

Fig. 3. Cyclic voltammograms of the Au/SAM/CNT/Hb electrode in the absence of H_2O_2 (solid line) and in the presence (dashed line) of 5×10^{-6} M in PBS with pH 7.0 at the scan rate of 0.2 V/s.

3.4. Optimal parameters of biosensors

Some experimental parameters for the construction of CNT/Hbs network and the detection of H_2O_2 with an Au/SAM/CNT/Hb-modified electrode were optimized in terms of polymerization cycle, pH, and applied potential. The number of electropolymerization cycle does effect on the fabrication of CNT/Hb network. Fig. S2 (in supplementary materials) shows the redox peak currents against CNT/Hb-modified electrodes, prepared by applying a variable number of electropolymerization cycles. As we can see, the redox peak current increases with the increase of electropolymerization up to 70 cycles and then saturated. This result is attributed to the higher amount of Hb presents in the CNT/Hb network electrode. Therefore, the application of 70 electropolymerization cycles was chosen to construct CNT/Hb network. Working under optimal applied potential at the working electrode gives fundamental contribution to achieve the lowest detection limit and avoid the electrochemical interferences. Therefore, the effect of applied potential on the response of the Au/SAM/CNT/Hb-modified electrode to 5×10^{-5} mol l^{-1} H_2O_2 was studied. The applied potential changes from 0.1 to −0.5 V (versus SCE) and the effect of the applied potential to the response of the Au/SAM/CNT/Hb-modified electrode to H_2O_2 was illustrated in Fig. S3 (in supplementary materials). The cathodic current intensity of H_2O_2 obtained at the Au/SAM/CNT/Hb-modified electrode increases with the negative shift of the operating potentials from 0.1 to −0.3 V; the current slightly decreases. At more negative potentials there might be a chance of interference reactions from other electroactive species, such as ascorbic acid or uric acid in the solution. As the maximum current response was obtained at −0.3 V and taking sensitive responses, effective avoiding interference and operational stability into consideration, −0.3 V was selected as the applied potential in subsequent experiments. Since the activity of the enzyme is pH dependent, investigation of the pH value of the detection solution on the performance of the biosensor is of great importance. Thus we have studied the effect of pH over the pH range of 3.0–9.0 in a PBS buffer solution containing 5×10^{-5} mol l^{-1} H_2O_2 at the optimum applied potential of −0.3 V. As shown in Fig. S4 (in supplementary materials), the current response increases in the pH range 3.0–6.0, then decreases, a small flat appeared at about pH 7.0–9.0. Since the maximum amperometric response is achieved at pH 6.0 of PBS solution, pH 6.0 was chosen as the optimized pH for following experiments. As previously reported, at the lower pH ranges, the denaturation of the biomolecules causes the low response of the biosensor (Kafi et al., 2008). In pH higher than 6, the adsorbed protein molecules are negatively charged, thus the electrostatic repulsion between the protein molecules on the electrode surface can decrease the saturation adsorption capacity of Hb (Wang et al., 2005).

3.5. Amperometric response of the biosensors

Fig. 4A illustrates a typical current–time curve of the Au/SAM/CNT/Hb-modified electrode upon the successive additions of a H_2O_2 solution in PBS at pH 6.0 at the applied potential of −0.3 V. As we can see, the Au/SAM/CNT/Hb-modified electrode exhibited a well defined reduction current proportional to the concentration of H_2O_2. The 95% of the steady-state current can be obtained at about 4–6 s by using the Au/SAM/CNT/Hb-modified electrode after the H_2O_2 solution was introduced. At the same time, much lower current responses were found at the Au/SAM/Hb-modified (a) with successive additions of H_2O_2. The resulting calibration

curve was linear in the range of 3×10^{-6} to 2×10^{-4} M (r=0.9998 and n=20) as shown in Fig. 4B. The sensitivity and the detection limit of the biosensor were calculated to be 0.29 μA/μM and 5×10^{-7} M at the S/N ratio of 3, respectively.

The apparent Michaelis–Menten constant (K_m), which gives an indication of the enzyme substrate kinetics for the biosensor, can be calculated from the electrochemical version of the Lineweaver–Burk plot (Kamin and Wilson, 1980).

$$\frac{1}{i_{ss}}=\frac{K_m^{app}}{i_{max}}\frac{1}{C}+\frac{1}{i_{max}} \quad (4)$$

Here i_{ss} is the steady-state current after the addition of substrate, i_{max} is the maximum current measured under saturated substrate condition, and C is the bulk concentration of the substrate. The K_m^{app} value was determined by analysis of the slope and intercept for the plot of the reciprocals of the steady-state current versus H_2O_2 concentration (Fig. 4B inset). The K_m^{app} value for the designed biosensor was found to be 0.19 mM, which is much smaller than that reported earlier (Shihong et al., 2007). Therefore, it can be said that the immobilized Hb in CNT/Hb network possesses higher enzymatic activity and the proposed electrode exhibits a high affinity for H_2O_2.

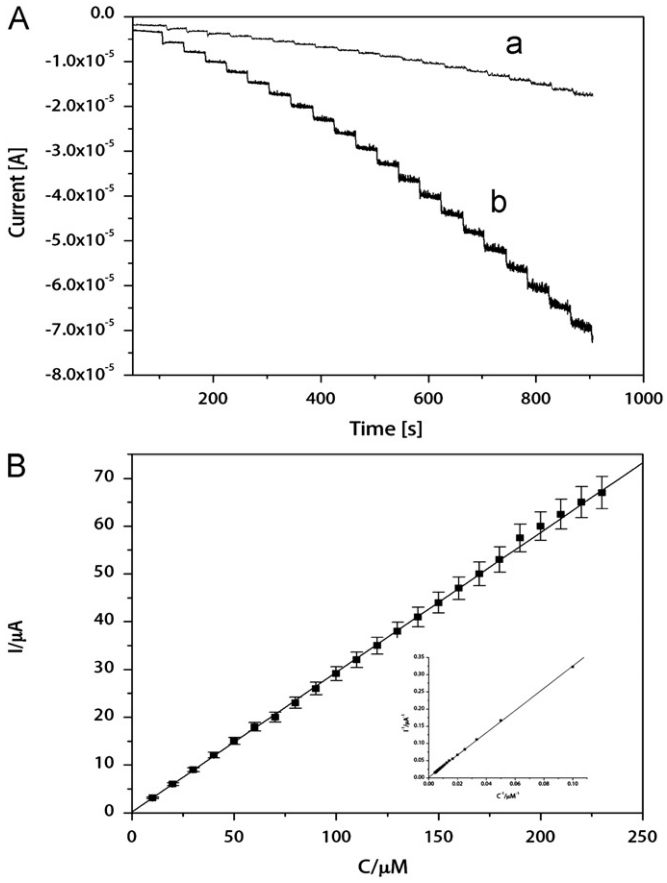

Fig. 4. (A) Typical Steady-state amperometric response of the Au/SAM/Hb electrode (a) the Au/SAM/CNT/Hb electrode (b) with the successive additions of 5×10^{-6} mol l^{-1} H_2O_2 in 0.1 mol l^{-1} PBS (pH 6.0) at the operating potential of −0.3 V. (B) Calibration plots for the Au/SAM/CNT/Hb electrode in the same experimental conditions. Inset shows the Lineweaver–Burk plot of $1/I_{ss}$ versus 1/C.

3.6. Reproducibility and stability of the biosensors

The long-term stability of this biosensor was also investigated. The Au/SAM/CNT/Hb-modified electrode was stored in PBS (pH 7.0) at 4 °C when not being in use. It retained 90% of its initial current response after 21 days. The repeatability of the sensor for current response was also examined. It was found that the relative standard deviation (RSD) was 3.75% for 10 successive measurements at a H_2O_2 concentration of 1×10^{-5} M. In addition, the electrode-to-electrode reproducibility was also studied between 5 different electrodes in above solutions, and the relative standard deviation was calculated to be 4.2%. Good reproducibility could be explained by the fact that the amount of immobilized in CNT/Hb network were consistent. The performance of the Au/SAM/CNT/Hb-modified electrode developed in this study was compared with other biosensors as shown in Table 1, showing that our proposed biosensor shows excellent performance in terms of long linearity, high stability and low detection limit.

4. Conclusions

In this work, the direct electrical contact of Hb and the Au electrode was achieved by constructing 3-D CNT/Hb networks. Hemoglobin was functionalized with 4-aminothiophenol by the primary modification of the lysine residues of the protein with the bifunctional reagent *N*-(ε Maleimidocaproyloxy) sulfosuccinimide ester, followed by the Michael addition of 4-aminothiophenol to the maleimide sites. And CNTs were functionalized with a mixed capping layer consisting of 4-aminothiophenol and mercaptoethanesulfonic acid. Finally, both functionalized CNTs and Hb were immobilized by coelectropolymerizaion procedure on the thiol-modified Au electrode in order make three-dimensional CNT/Hb network. The CNTs have provided conductivity to the CNT/Hb network, the bis-aniline bridging units acted as electron-mediating components for the electron transfer between the enzyme redox centers and the electrode. At the same time, high surface area of the CNTs yielded close proximities between the redox centers of Hb and the electron relay units, and this led to the effective wiring of the Hb with the electrode. At the end, the preparation of the electrodes by 3-D CNT/Hb networks reveals a further technological advantage as it allows the modification of the working electrode with the bioelectrocatalytic matrix and high throughput manufacturing of miniaturized biosensors. Detailed experiments in terms of optimal parameters and real sample analysis are underway in our laboratory and will be reported in due course.

Table 1
Comparison of the performance of different H_2O_2 biosensors (HRP=Horseradish peroxide; Hb=Hemoglobin and LOD=Limit of Detection).

Modified electrode	Linear range (M)	LOD (μM)	Stability	References
Hb in CNT/Polymer	4.0×10^{-5} to 7.2×10^{-4}	3.2	95% 14 days	Li et al., 2012
Hb in Au NP/TiO_2	5.0×10^{-5} to 1×10^{-3}	0.6	Not reported	Wei et al., 2011
Hb in Au-nano-particle	1.0×10^{-5} to 7×10^{-3}	4.5	95% 40days	Zhang and Li, 2004
HRP in AU nano-seed	4.1×10^{-5} to 6.3×10^{-4}	5.9	90% 14 days	Wang et al., 2010
Hb in carbon nanotube	2.1×10^{-4} to 9.0×10^{-4}	9	Not reported	Zhao et al., 2005
Hb in TiO_2 nanotube	4×10^{-6} to 6.4×10^{-5}	4.6	90% 21days	Zheng et al., 2008
HRP in carbon nanotube	3×10^{-5} to 1×10^{-2}	12.89	Not reported	Chen and Dong, 2007
In this work (Hb in crosslinked 3D networks)	3×10^{-6} to 2×10^{-4}	0.5	90% 21 days	

Acknowledgments

A.K.M. Kafi acknowledges the Henry Bertie and Florence Mabel Gritton Postdoctoral Fellowship, the University of Sydney.

Appendix A. Supplementary materials

Supplementary materials associated with this article can be found in the online version at http://dx.doi.org/10.1016/j.bios.2012.10.040.

References

Baravik, I., Tel-Vered, R., Oded, O., Willner, I., 2009. Langmuir 25, 13978–13983.
Bard, A.J., Faulkner, L.R., 1980. Electrochemical Methods. Wiley, New York.
Chen, H., Dong, S., 2007. Biosensors and Bioelectronics 22, 1811–1815.
Dorst, B.V., Mehta, J., Bekaert, K., Martin, E.R., Coen, W.D., Dubruel, P., Blust, R., Robbens, J., 2010. Biosensors and Bioelectronics 26, 1178–1194.
Fruk, L., Kuo, C.H., Torres, E., Niemeyer, C.M., 2009. Angewandte Chemie—International Edition 48, 1550–1574.
Gooding, J.J., Wibowo, R., Liu, J., Yang, W., Losic, D., Orbons, S., Mearns, V., Shapter, F.J., Hibbert, D.B., 2003. Journal of the American Chemical Society 125, 9006–9007.
He, P., Dai, L., 2007. BioMEMS and Biomedical Nanotechnology. Springer, US 171.
Holland, J.T., Lau, C., Brozik, S., Atanasso, P., Banta, S., 2011. Journal of the American Chemical Society 133, 19262–19265.
Kafi, A.K.M., Guosheng, W., Chen, A., 2008. Biosensors and Bioelectronics 24, 566–571.
Kafi, A.K.M., Asieh, A., Wang, J., Thomas, D.F., Chen, A., 2010. Biosensors and Bioelectronics 25, 2458–2463.
Kamin, R.A., Wilson, G.S., 1980. Analytical Chemistry 52, 1198–1205.
Katz, E., Heleg-Shabtai, V., Willner, B., Willner, I., Bєuckmann, A.F., 1997. Bioelectrochemistry and Bioenergetics 42, 95–104.
Kotani, H., Ohkubo, K., Crossley, M.J., Fukuzumi, S., 2011. Journal of the American Chemical Society 133, 11092–11095.
Laviron, E., 1979. Journal of Electroanalytical Chemistry 101, 19–28.
Li, Y., Huanga, F., Luob, Z., Xub, B., Wanga, X., Li, F., Wanga, F., Huanga, L., Li, S., Li, Y., 2012. Electrochimica Acta 74, 280–287.
Ligler, F.S., 2009. Analytical Chemistry 81, 519–526.
Liu, G.Z., Paddon-Row, M.N., Gooding, J.J., 2007. Electrochemistry Communications 9, 2218–2223.
Ma, H.Y., Hu, N.F., Rusling, J.F., 2000. Journal of Electroanalytical Chemistry 16, 4969–4975.
Patolsky, F., Weizmann, Y., Willner, I., 2004. Angewandte Chemie—International Edition 43, 2113–2117.
Raitman, O.A., Katz, E., Bückmann, A.F., Willner, I., 2002. Journal of the American Chemical Society 124, 6487–6496.
Sardesai, N.P., Barron, J.C., Rusling, J.F., 2011. Analytical Chemistry 83, 6698–6703.
Shihong, C., Yuan, R., Chai, Y., Zhang, L., Wang, N., Li, X., 2007. Biosensors and Bioelectronics 22, 1268–1274.
Turner, A.F.P., 2007. American Association for the Advancement of Science 290, 1315–1317.
Wang, C.H., Yang, C., Song, Y.Y., Gao, W., Xia, X.H., 2005. Advanced Functional Materials 15, 1267–1275.
Wang, J., 2005a. Small 11, 1036–1043.
Wang, J., 2005b. Electroanalysis 17, 7–14.
Wang, J., 2008. Chemical Reviews 108, 814–825.
Wang, L., Wang, E., 2004. Electrochemistry Communications 6, 225–229.
Wang, Y., Ma, X., Wen, Y., Xing, Y., Zhang, Z., Yang, H., 2010. Biosensors and Bioelectronics 25, 2442–2446.
Wang, Y., Joshi, P.P., Hobbs, K.L., Johnson, M.B., Schmidtke, D.W., 2006. Langmuir 22, 9776–9783.
Wei, N., Xin, X., Du, J., Li, J., 2011. Biosensors and Bioelectronics 26, 3602–3607.
Willner, I., Katz, E., 2005. Bioelectronics. WILEY-VCH Verlag GmbH & Co. KGaA, Weinheim.
Willner, I., Heleg-Shabtai, V., Blonder, R., Katz, E., Tao, G., Bєuckmann, A.F., Heller, A., 2009. Journal of the American Chemical Society 118, 10321–10322.
Wiilner, I., Katz, E., Willner, B., 1997. Electroanalysis 9, 965–977.
Willner, I., Willner, B., 2001. Trends in Biotechnology 19, 222–230.
Xiao, Y., Patolsky, F., Katz, E., Hainfeld, J.F., Willner, I., 2003. Science 299, 1877–1881.
Yan, Y.M., Baravik, I., Yehezkeli, O., Willner, I., 2008. Journal of Physical Chemistry C 112, 17883–17888.
Yang, W., Thordarson, P., Gooding, J.J., Ringer, S.P., Braet, F., 2007. Nanotechnology 18, 412001–412012.
Yang, W., Zhou, X., Zheng, N., Li, X., Yuan, Z., 2011. Electrochimica Acta 56, 6588–6592.
Yehezkeli, O., Yan, Y.M., Baravik, Tel-Vered, I., Willner, I., 2009. Chemistry—A European Journal 15, 2674–2679.
Zayats, M., Willner, B., Willner, I., 2008. Electroanalysis 20, 583–601.
Zheng, W., Zheng, Y.F., Jin, K.W., Wang, N., 2008. Talanta 74, 1414–1419.
Zhao, Y.D., Bi, Y.H., Zhang, W.D., Luo, Q.M., 2005. Talanta 65, 489–494.
Zhang, W.J., Li, G.X., 2004. Analytical Sciences 20, 603–610.